Interference by Rain Scatter

Robert K. Crane
Thayer School of Engineering
Dartmouth College

Introduction.

Rain scatter has long been recognized as a mechanism for the generation of co-channel interference between microwave systems operating at the same frequency. Based on the results of the NASA Virginia Precipitation Scatter Experiment [Crane, 1973], the international radio regulations were modified in the early 70's to force a consideration of the potential for interference by rain scatter as a part of the frequency assignment process (coordination). At the time the rain coordination procedure was introduced, the inadequacy of our knowledge of the statistics of the spatial structure of precipitation was recognized and only a preliminary, ad hoc model for the extension of the coordination procedures to attenuating frequencies could be included to complete the model for the radio regulations [Crane, 1974]. Since that time, a number of equally poor model modifications have been introduced by the International Radio Consultative Committee (CCIR) to cover the acknowledged problem of extension to higher frequencies. In this study for the NASA Propagation Program, we are employing data from a measurement program by the Thayer School of Engineering, Dartmouth College and the U. S. Air Force, Rome Air Development Center (RADC) to supplement a simulation study for the development of an improved model for the prediction of interference level fields at attenuating frequencies.

Frequency allocations personnel in European countries have complained about the rain coordination procedure ever since it was incorporated into the radio regulations. The often heard complaint is that rain scatter does not exist. No occurrences of interference by rain scatter have ever been documented. The problem, however, is not the existence of rain scatter but the recognition of an occurrence of interference by rain scatter at the fraction of a year for which such interference is allowed. As shown in Figure 1, scattering by rain exists and the observations are in close agreement with model predictions at non-attenuating frequencies. The measured reflectivities at a 3 km height (10K-Eastville and 10K-Ft. Lee) are within one dB (the measurement system uncertainty) of the values predicted on the basis of rain rate measurements made at the surface under the scattering volume (Rain Gauge). The bistatic reflectivity factor observations were 3 dB below the values predicted for the Virginia rain climate (Global climate D2 [Crane,1985a]). In this case, the discrepancy is due to a difference between the observed and predicted surface rain rates but not to the prediction model when surface rain rate measurements are used. Sakagami [1980] made observations of rain scatter over a two year period at a frequency of 6.72 GHz on a 55.2 km forward scatter path near Tokyo and reported good agreement between the observed reflectivities at a height of 2.3 km and equiprobable reflectivity values estimated from surface rain rate measurements. In this experiment adjustments were made for attenuation by rain on the forward scatter path from line-of-sight attenuation measurements to an elevated antenna.

The Virginia Precipitation Scatter Experiment (Figure 1) employed simulated terrestrial and earth-space communications paths. The common volumes for rain scatter coupling between the simulated communications links were located at heights of 10K feet (3 km) and 20K feet (6 km). Terrestrial paths from two separated transmitter locations, Eastville and Ft. Lee, VA, were used to illuminate the scattering volumes along the slant path to the receiver site at the NASA Langley Research Center. Distances from the antennas to the common volume ranged from 13 to 78 km. For the simulated communications links, a transmission loss in

excess of 162 dB would have been required to prevent interference. This transmission loss corresponds approximately to an equivalent reflectivity factor of 22 dBZ_e. For the data displayed in the figure and the communication link parameters assumed for the simulation, interference would have been recorded each time rain with an equivalent rate in excess of 0.5 mm/h occurred within the common volume. From these data it is evident that rain scatter does occur and has the potential for causing interference.

The intervals with interference caused by rain would be brief, corresponding to the occurrences of hydrometeors within the scattering volume at the fractions of a year indicated in Figure 1. Because the procedures in the radio regulations now guard against interference at the percentages of the year corresponding to most of the data in the figure (the assumptions used for the interference simulation were not valid after the 1971 World Administrative Radio Conference which adopted the coordination procedures for rain), the only time a report of excessive interference might be brought to the attention of the frequency allocations community is for rain events with rates significantly in excess of the values corresponding to annual percentages ranging from 0.05 to 0.001 %. Such rains occur with very brief durations and probably would go unnoticed in comparison with the much longer duration interference events that occur due to failures in the CCIR duct propagation prediction model. The interference events, although unnoticed from a practical point of view, still produce a sufficient disruption in service to affect link reliability.

Extension to Higher Frequencies.

The CCIR models for the extension of interference prediction and rain coordination procedures to higher frequencies have varied with time. In the early 70's, a conservative model (favoring the current assignees) was recommended. It considered only attenuation by rain within the scattering volume common to the intersecting antenna beams (the common volume) and ignored any attenuating hydrometeors outside the scattering volume [Crane, 1974]. More recently a series of models have been recommended by the CCIR that try to include statistically the simultaneous occurrences of rain inside the common volume and along the paths from the common volume to the transmitters and receivers. These procedures have tended to be less conservative. Unfortunately, little experimental work on rain scatter interference at the higher frequencies has been reported since the Virginia Precipitation Scatter Experiment. One set of long term observations is now available from Japan at 14 GHz [Awaka et al., 1984].

When it was realized that the original interference estimation bound was too conservative, CCIR Study Group 5 s were revised to model the inclusion of an attenuation estimate. The model now predicts too high a transmission loss; the model is now not conservative enough. Awaka [1984] correctly placed the cause for the failure of the model on an inadequate treatment of the statistical relationship between the scattering process in the common volume of the antenna patterns of the potentially interfering systems and the attenuation along the paths between the common volume and the antennas. He suggested the use of a joint log-normal statistical model for predicting the transmission loss when both the scattering and attenuation processes were important.

The problem arises from the competing effects of scattering and attenuation. Figure 2 displays the predictions of the two-component rain model [Crane, 1982] after modification to estimate the expected received power when rain is present in the common volume and attenuation is present along the paths from the antennas to the common volume. It is for the scattering geometry of the Kashima-Inubo and Kashima-Hiraiso measurements reported by Awaka et al. [1984]. Simultaneous bistatic scattering observations from a scattering volume at

a height of 2 km were made at Inubo and Hiraiso. The reflectivity factor for scattering in the absence of attenuation is given by the curves labeled "Rain Gauge" for simultaneous surface rain rate measurements at the transmitter site and "Climate D1" for estimates based on the Global rain climate model [Crane, 1985a]. For this location, the climate model closely approximated the gauge measurements.

The two-component predictions are for the backscatter and forward scatter geometries [Crane, 1974] and the D1 climate rain rate model. The effect of attenuation is evident in the figure. The backscatter geometry models (Back H for Hiraiso and Back I for Inubo) most closely reproduce the observations. Attenuation in the debris component of the two-component rain model causes the plateau in the forward scatter curve at 0.03 % of the year. The nearly 125° and 86° scattering angles for the Hiraiso and Inubo paths were best modeled by backscatter.

Excellent agreement is evident between the two-component model predictions and the 14.3 GHz observations over the 0.0001 to 1 % of the year range. A small discrepancy is evident at higher percentages when the surface rain rate observations depart from the climate model predictions. If the actual surface rain rate values had been used, this discrepancy would disappear. The model adequately handles the simultaneous occurrences of scattering and attenuation for attenuation values up to about 8 dB. No long term observations are available in the literature to test the model over a wider range of attenuations.

Awaka et al [1983] reported bistatic scatter measurements at 34.8 GHz for the summer season for the Hiraiso-Kashima path. These limited duration measurements are displayed in Figure 3 along with the forward and backscatter two-component model predictions for the D1 climate region. The forward scatter model includes sufficient attenuation to suppress the debris component scattering while the cell component rises to within a few dB of the observations at percentages less than 0.01%. The backscatter model again works best and is within 2 dB for less than 0.3% of the summer months. In this case the scattering angle was 19° which, by the CCIR model, should classify the path as forward scatter instead of backscatter.

The Two-Component Rain Scatter Model.

The two-component rain model has been found useful for the prediction of attenuation on terrestrial and slant paths [Crane, 1985a,b]. We now apply it to the problem for which it was originally developed. The model breaks the rain occurrence problem into two parts, the occurrence of cells (isolated) and of widespread rain (debris). The occurrence of either is assumed to be independent of the other. The attenuation prediction model calculates the rain rate needed to produce the desired value of attenuation by each process then sums the probability of the occurrence of cells or debris with the appropriate rain rate anywhere on the path. For application to rain scatter we start with an equivalent rain rate within a cell or debris region (width) located randomly within the common volume created by the intersection of the antenna patterns. We know the probability for the occurrence of that rain rate for either the cell or debris process. We next calculate the attenuation that would occur on the adjacent segments of the propagation path using the cell and debris extent (width) values. If we have a backscatter geometry the attenuation within the common volume is not included but is incorporated in the manner described by Crane [1974].

The probability density for the occurrence of specified values of equivalent reflectivity (or of transmission loss) is then calculated from the probability density for rain rate. The final cumulative probability distribution is then found by integrating the density. The use of

probability densities is required because the relationship between rain rate in the common volume and transmission loss is not monotonic. For the forward scatter case, the cell or debris with or the total path length, whichever is smaller is used for the calculation of attenuation. In the backscatter case, the random locations of the cell or debris structures along the path are used to vary the attenuation in the calculation of the probability density values for the effective reflectivity factor. The inclusion of attenuation as a random process in the backscatter case makes it applicable for all the scattering geometries except those very close to a purely forward scatter case (scattering angle < 5° say).

The Forward Scatter Case.

The Prospect Hill to Mt. Tug troposcatter path used by RADC and Dartmouth for communications studies is a transhorizon propagation path with a scattering angle of 2°. In the context of the two-component rain scatter model, it qualifies as a forward scatter path. In this case, the effect of attenuation is maximized relative to the effect of scattering. Model predictions are given in Figure 4. Attenuation is of little consequence at 5 GHz but is extremely important at 16 GHz. The Ku-band (15.73 GHz) predictions show the plateau produced by debris component attenuation. For rain, the Ku-band received power should not exceed -84 dBm except for very brief intervals when it will increase to -83 dBm. Simultaneous measurements at C-Band should show signal level variations from -84 to -73 dBm over the 0.01 to 0.3 % range when the Ku band signal saturates at -84 dBm. These predictions apply to the cumulative distribution of received signal levels, not to the instantaneous received signal time series.

Figure 5 depicts the cumulative distributions for 49 hours of observations during the spring and summer of 1987. The distributions are for a) clear weather (troposcatter) conditions (11 hrs.), b) all observations (49 hrs.), c) all observations with rain (34 hrs) and d) observations with light rain (24 hrs.). The troposcatter only curves (a) are in close agreement with predictions based on clear air scattering by atmospheric turbulence (not using the CCIR models which do not correctly estimate troposcatter field strengths at frequencies above about 10 GHz). The all rain data (c) show a upper level of -84 dBm at Ku-band (dashed curves in Figures 5 through 7) in apparent agreement with the two-component model predictions but this interpretation is not supported by the C-band (5 GHz) data. If the Ku-band observations are about -84 dBm, the simultaneously occurring C-band measurements should be above -84 dBm. However, the C-band observations are all less than -90 dBm.

Figure 6 depicts a) the cumulative distribution, b) the received power time series, c) the power spectrum for received power variations (in dB) and d) the instantaneous differences between Ku and C band measurements. The power spectra (a) display the $k^{-5/3}$ behavior typical of rain when averaged over spatial scales greaterthan~10 km. The time series (b) and (d) show variations in received power typical of light rain (C-band levels are for reflectivities less than 16 dBZ peak). At ku-band, the signal levels exceed those predicted for rain even if no attenuation occurs along the path. These results suggest that more must be involved in the modeling of scattering by rain in the forward direction (and perhaps other directions, the success of the model as shown in Figures 2 and 3 notwithstanding).

Figure 7 displays simultaneous observations at C- and Ku-band for occurrences of light rain. In this case (September), the observations are consistent with a rain scatter interpretation with reflectivities less than 23 dBZ as observed at C-band.

Conclusions.

The data from Japan and the US (the Virginia Precipitation Scatter Experiment) show excellent agreement between the two-component rain scatter model predictions and bistatic scatter measurements. In employing the model, all the scattering geometries should be classified as "backscattering" as defined by Crane [1974]. The forward scatter model should only be used for great circle paths with both antennas pointed at the horizon and at each other in a typical troposcatter communication system geometry. The forward scatter model can also be used for main-lobe, side-lobe coupling when one antenna is pointed toward the other along the great circle path.

The forward scatter observations made over the Prospect Hill - Mt Tug path show that the two-component model is incomplete. Much stronger signals were observed at Ku-band than expected based on simultaneous C-band measurements. The discrepancies may be due to: 1) scattering by ice/snow at height (possible in April (Figure 6) at the 1 km height of the scattering volume), 2) the coherent effects of turbulent fluctuations in the hydrometeor number densities and 3) errors in the modeling of the statistical relationship between attenuation along the path and scattering in the common volume.

References.

Awaka, J. [1984]: A prediction method for the received power from rain scatter, *Radio Science*, **19**, 643-651.

Awaka, J., T. Kozu, K. Nakamura, and H. Inomata [1984]: Experimental Results on Bistatic Rain Scattering at 14.3 GHz, *IEEE Trans. Antennas and Propagation*, **AP-32,** 1345-1350.

Awaka, J., K. Nakamura, and H. Inomata [1983]: Bistatic Rain-Scatter Experiment at 34.8 GHz, *IEEE Trans. on Antenna and Propagation*, **AP-31,** 693-698.

Crane, R. K. [1985a]: Comparative evaluation of several rain rate attenuation prediction models, *Radio Science*, **20**, 843-863.

Crane, R. K. [1985b]: Evaluation of global and CCIR models for estimation of rain rate statistics, *Radio Science*, **20**, 865-879.

Crane, R. K. [1982]: A two-component rain model for the prediction of attenuation statistics, *Radio Science*, **17**, 1371-1387.

Crane, R. K. [1974]: Bistatic Scatter from Rain, *IEEE Trans. Antennas and Propagation*, **AP-22**, 312-320.

Crane, R. K. [1973]: Virginia Precipitation Scatter Experiment - Data Analysis, NASA/GSFC X-750-73-55, Goddard Space Flight Center.

Sakagami, S. [1980]: Some Experimental Results on Bistatic Scatter from Rain, *IEEE Trans. Antennas and Propagation*, **AP-28**, 161-165.

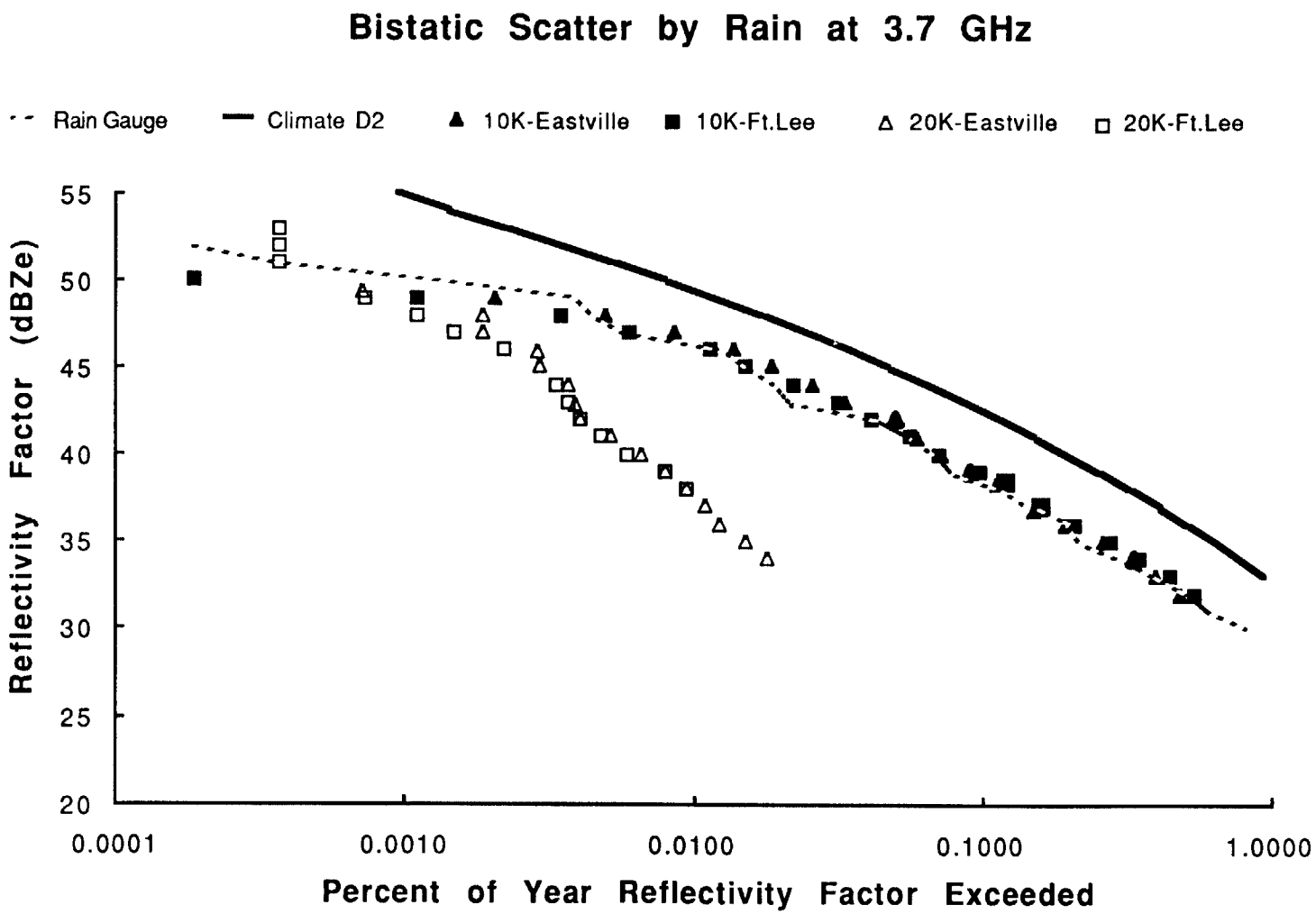

Figure 1 Bistatic scatter measurements October 3, 1970 - October 2, 1971 Virginia Precipitation Scater Experiment [Crane, 1973].

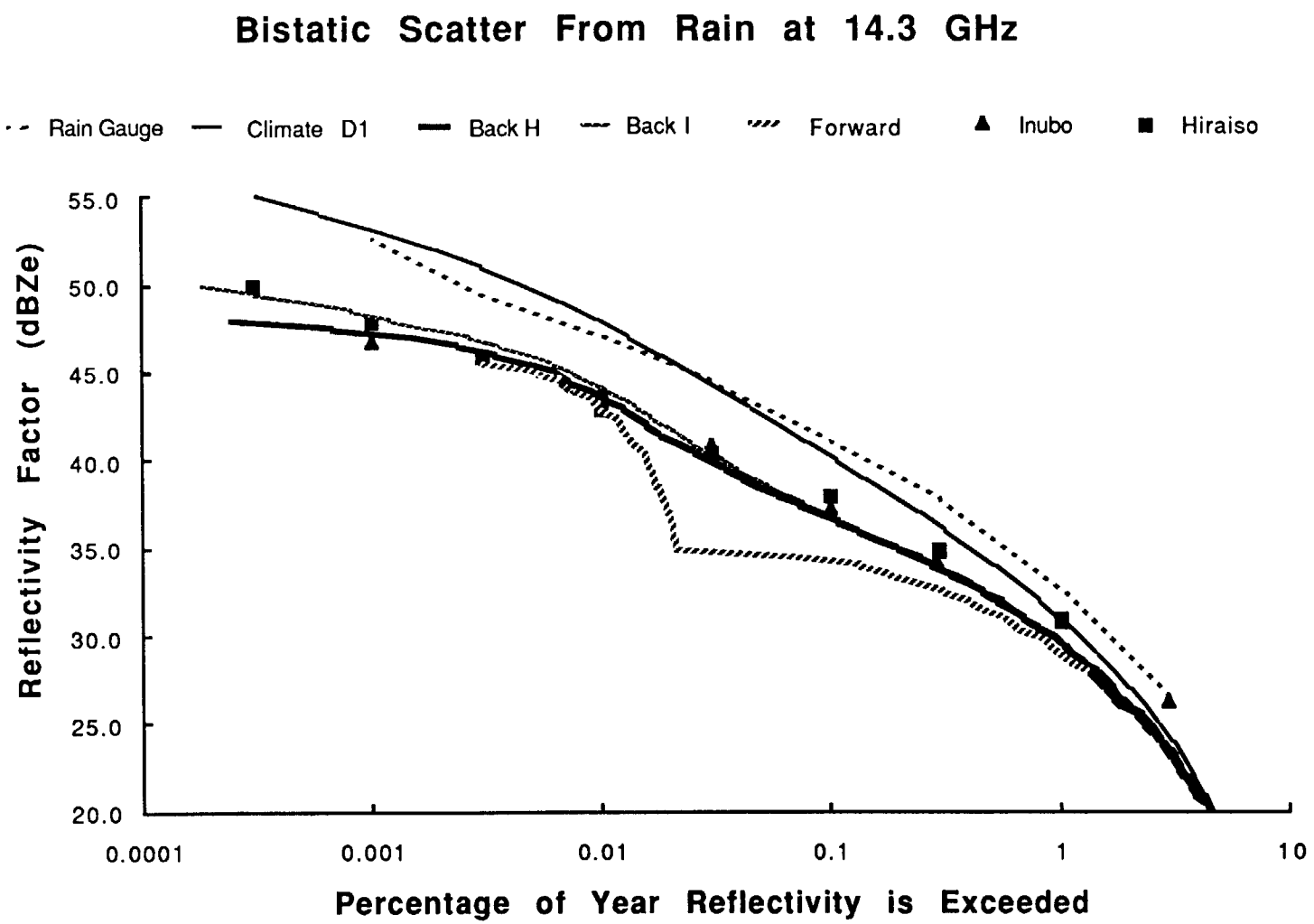

Figure 2 Bistatic scatter measurements May 9, 1981 - May 8, 1982 Kashima, Japan [Awaka et al., 1984].

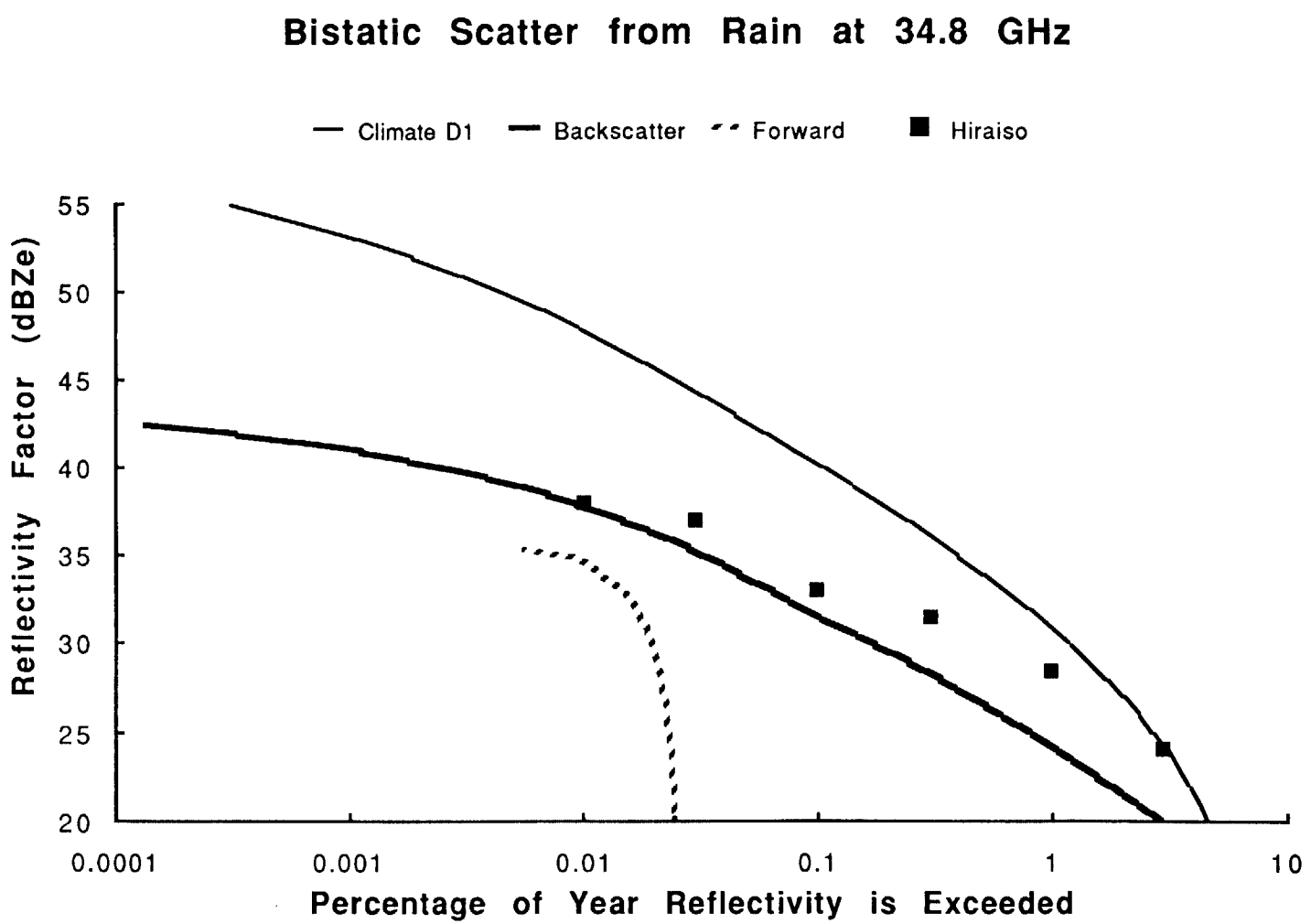

Figure 3 Bistatic scatter measurements June 9 - September 26, 1980 Kashima, Japan [Awaka et al., 1983].

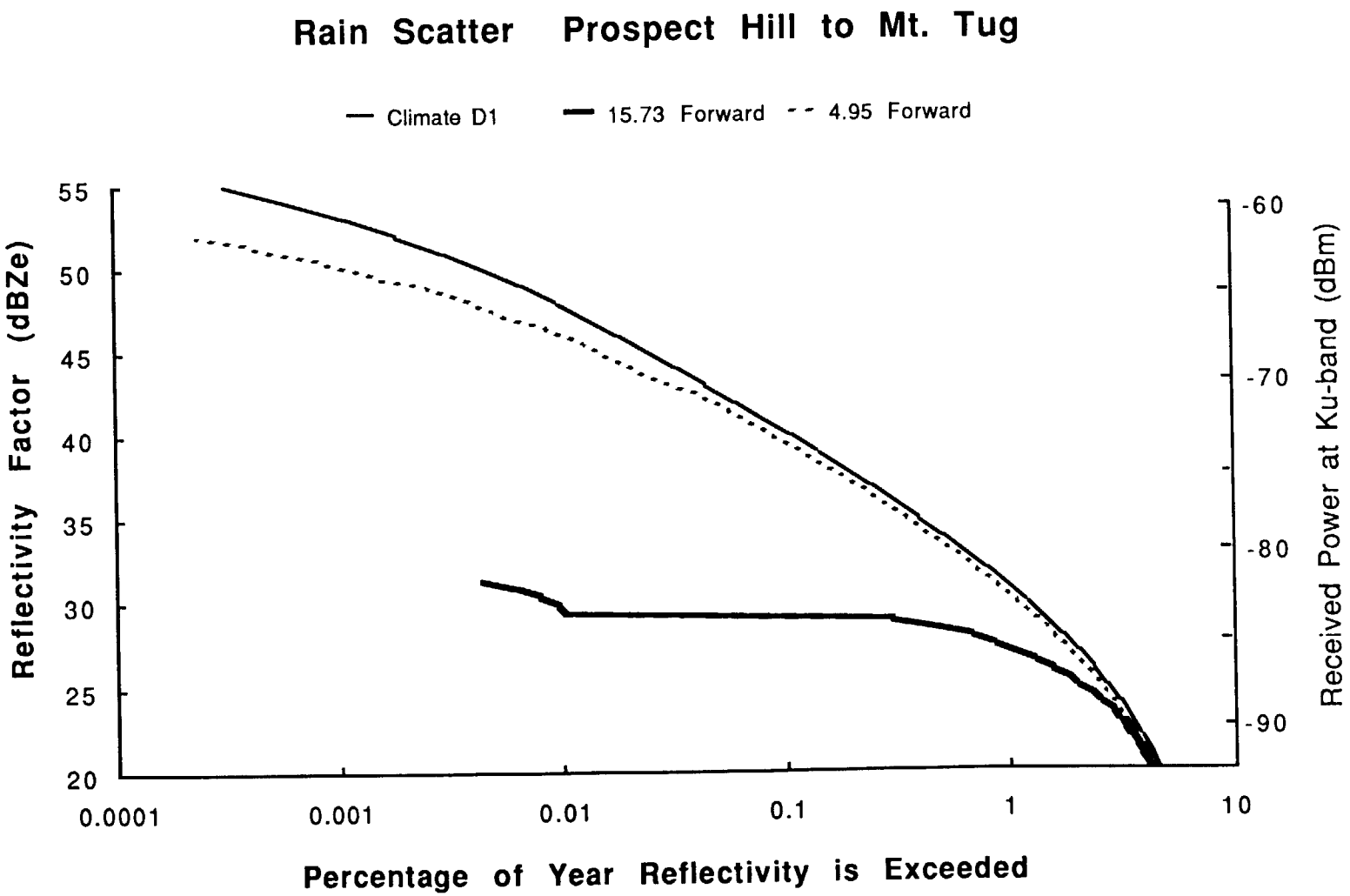

Figure 4 Model predictions for the Prospect Hill - Mt. Tug path

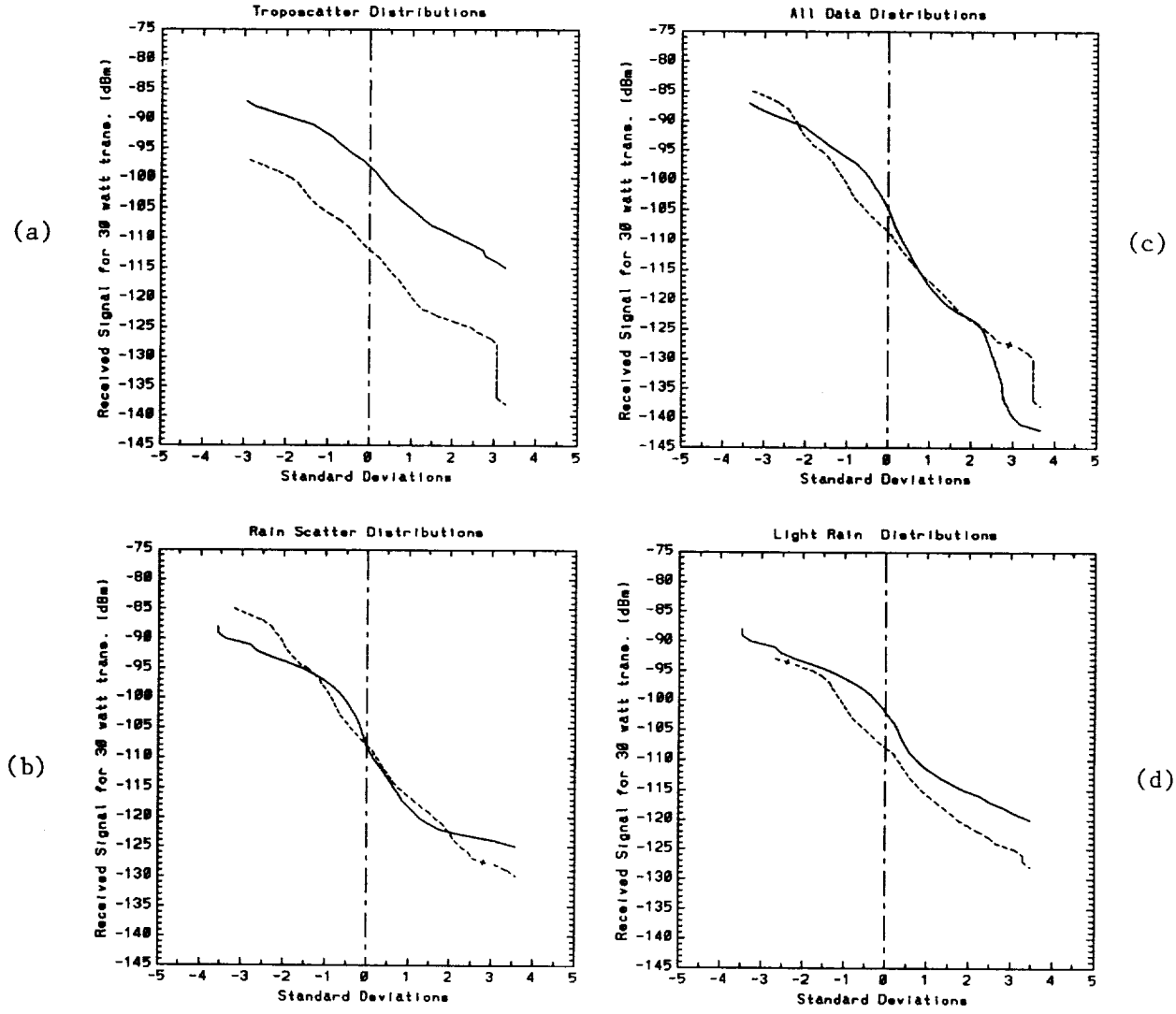

Figure 5. Cumulative Distribution for 49 hours of observations on the the Prospect Hill to Mt. Tug troposcatter path. (Solid curves for C-band and dashed curves for Ku-band).

(a)

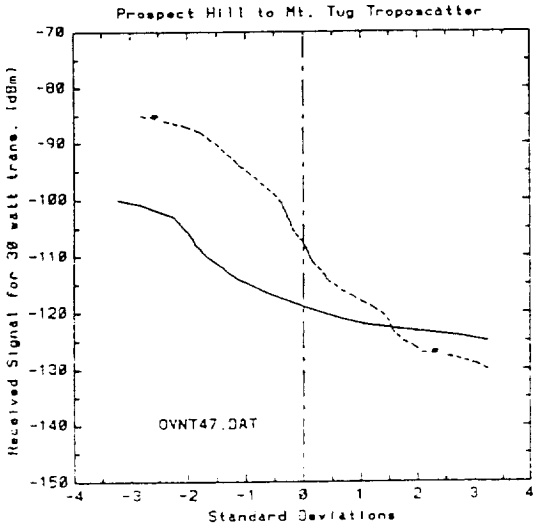

(c)

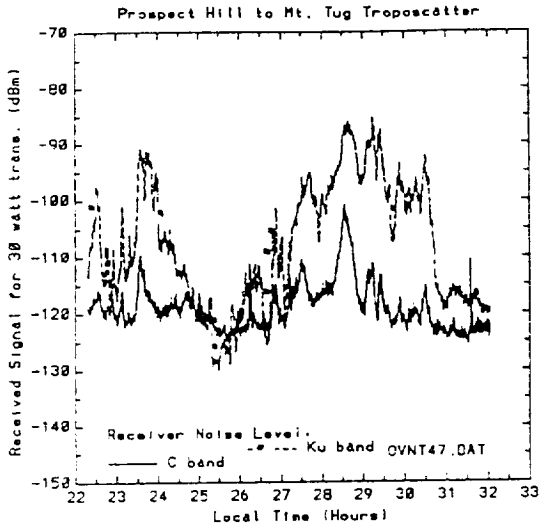

(b)

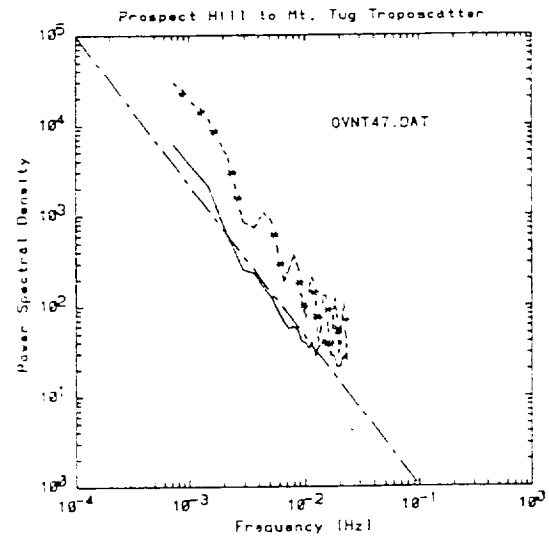

(d)

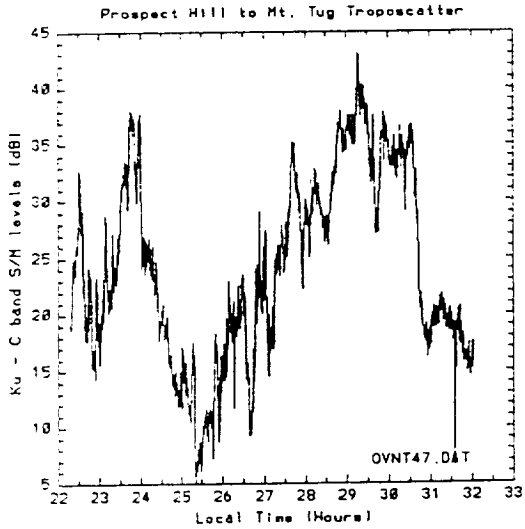

Figure 6. Observations in rain, April 6 and 7, 1987.

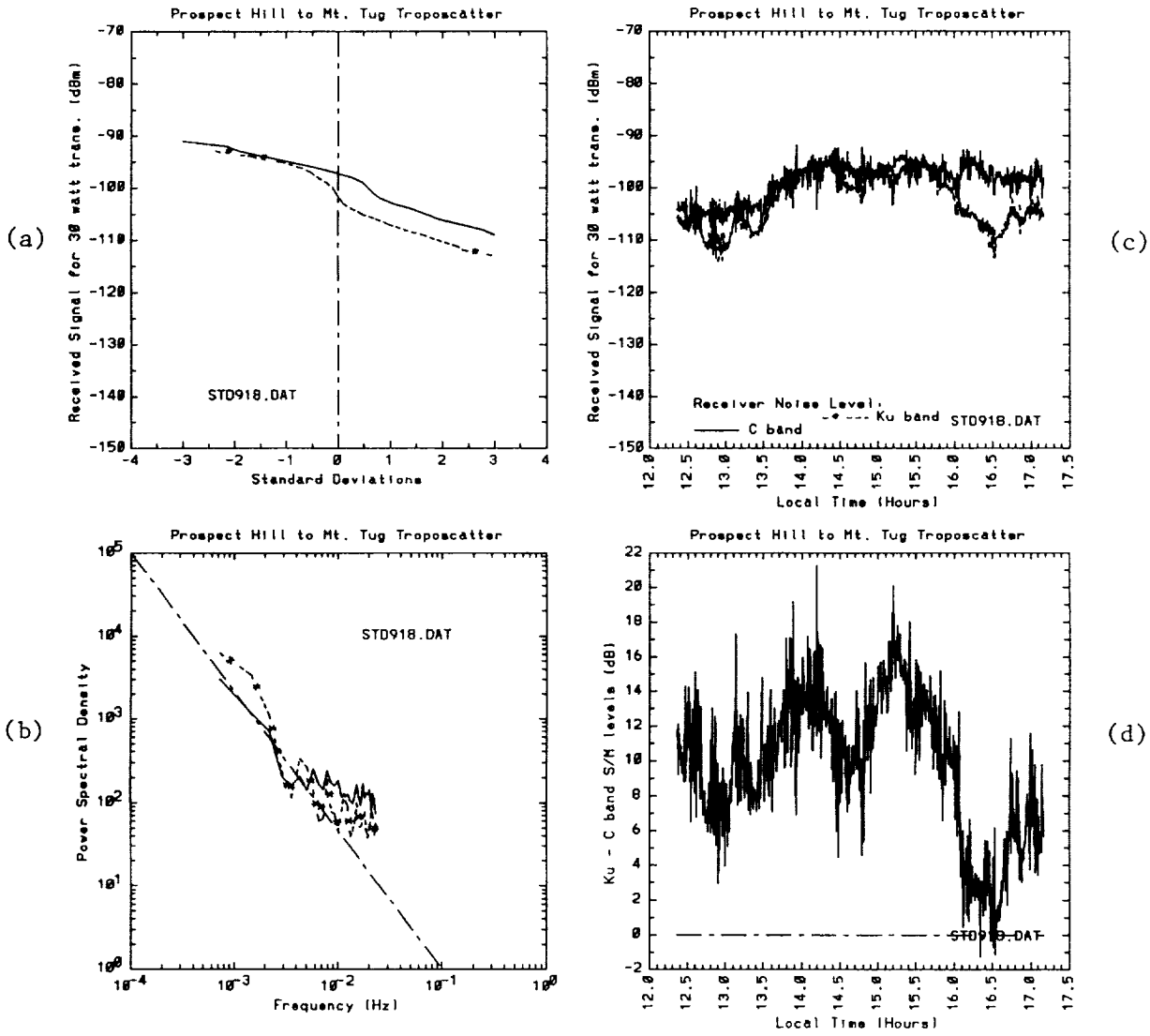

Figure 7. Observations in light rain, September 18, 1987.